Investigation of Magnetic Resonance Coupling Circuit Topologies for Wireless Power Transmission

Jingchen Wang[1] | Mark Leach[1] | Eng Gee Lim[1] | Zhao Wang[1] | Yi Huang[2]

[1]The department of Electrical and Electronics Engineering, Xi'an-jiaotong Liverpool University, Suzhou 215123, P. R. China.
[2] The department of Electrical Engineering and Electronics, The University of Liverpool, Liverpool L69 3BX, U.K

Correspondence
Mark Leach, Department of Electrical and Electronics Engineering, Xi'an-jiaotong Liverpool University, Suzhou 215123, P. R. China.
Email: mark.leach@xjtlu.edu.cn

Abstract
Magnetic resonance coupling circuits have four general topologies, however, there is a lack of comprehensive theoretical analysis together with experimental verification on each of these topologies in relation to their attractiveness for wireless power transfer. This paper aims to provide both of these for each of the four topologies in order to fully understand the differences between them and allow the selection of the correct type based on system requirements. In addition, one of the problems associated with the resonance coupling method is the phenomenon of frequency splitting, which can lead to a high-power transfer efficiency but low load power at the resonant frequency. Reasons for frequency splitting and methods of circumventing the problem will be illustrated in this paper. Of the four topologies Series-Parallel (SP) (input-output circuit configuration) is the most efficient for the realization of a wireless power transfer system with a large load impedance, in terms of achieving both a high-power transfer efficiency and high load power.

KEYWORDS

wireless power transmission, magnetic resonance coupling, topologies selection, frequency splitting.

1 | INTRODUCTION

Wireless and portable mobile devices have become commonplace, however keeping these devices active and supplied with power is a continual and critical problem. Battery charging is currently dominated by wired technology, which requires a wired power plug to be connected to an electrical wall outlet. Importantly, wireless power transfer (WPT), as a promising and innovative technology, is able to achieve the same goal whilst avoiding the limitations of wires. WPT technologies are revolutionizing the way energy is transferred and has the potential to make our lives truly "wireless". Recently, WPT technologies have been applied to charge batteries in medical sensors and implanted devices, where battery replacement is not convenient [1-3]. They have also been applied to recharge mobile devices (e.g., cell phones, tablets, laptops) [4-5] and electric/hybrid vehicles [6-8].

Generally speaking, WPT technologies can be categorised into radiative WPT (via electromagnetic radiation) and non-radiative WPT (via inductive or magnetic resonant coupling). Radiative wireless charging adopts electromagnetic waves, typically RF waves or microwaves, as a medium to deliver energy in the form of radiation. The energy is transferred based on the electric field of an electromagnetic wave. When the RF density exposure is high, there are safety issues for human beings. This method is suitable for broadcast applications over a long effective charging distance (kilometre-range). Alternatively, non-radiative WPT, which is based on the coupling of the magnetic-fields of two (or more) coils, can be used for energy transmission over short distances, typically within the coils' dimension [9]. The advantages and disadvantages between non-radiative WPT and radiative WPT have been discussed in [10-11].

Nowadays, the magnetic resonance coupling (MRC) method is widely used for WPT due to its high transfer efficiency since it was put forward by Kurs *et al* in Massachusetts Institute of Technology using self-resonant coils in 2007 [12]. Even though the WPT technique provides some advantages with respect to research and commercial usage, the magnetic coupling approach, as a modernised method, still has some theoretical issues and practical challenges which need to be addressed and overcome [13-14]. In [15-17], secondary series-and parallel-compensated WPT circuits were compared to investigate the influence of load impedance on power transfer efficiency. However, sufficient practical verifications of the theory through published experimental results were not provided. Despite all four topologies of the WPT circuit being studied in [18-20], comparison between the four topologies was limited, with no criteria provided as to which topology was most appropriate for a given system. For example, literatures on design and optimization of wireless power links initially used parallel-primary and parallel secondary circuits [21-23]. Later most references focused on series-primary and series-secondary circuits for wireless power transfer [24-26]. However, the phenomenon of frequency splitting [27-29] can easily appear when series-primary and series-secondary circuits leading to low power transfer efficiency. To enhance power transfer efficiency at certain frequencies, there are some techniques such as impedance matching [30-31], high Q-factor coil designs [32-33] and load optimization [34]. However, the load cannot be optimized to enhance power transfer efficiency because it is

normally fixed. Therefore, it is necessary and crucial to focus on a solution to design a suitable WPT system with high power transfer efficiency for applications with fixed loads.

In this work, comprehensive investigations on four topologies for MRC-WPT have been performed, including theoretical analysis and experimental verifications. From the viewpoint of the primary and secondary circuits, a detailed introduction and theoretical analysis of the four topologies for MRC-WPT is provided in Section II. Solutions to designing an optimal WPT system and a description of the experimental designs are delivered in Section III. Section IV offers related experimental verifications and the investigation of the phenomenon of frequency splitting in terms of circuit parameters and power transfer efficiency. Conclusions regarding MRC-WPT, including a comparison between the four topologies and selection of the most appropriate topology for a given wireless power transfer system is highlighted in Section V.

2 | THEORETICAL ANALYSIS OF TOPOLOGY

Resonance is a trend where a physical system subjected to its natural frequency, will tend to absorb energy at that frequency. In other words, it is a phenomenon in which, when one object vibrates it will cause another with the same resonant frequency to vibrate, such as sound at a specific frequency causing a tuning fork with that frequency to vibrate. In this regard resonance can be used to transfer energy. Electromagnetic resonance is used widely in electromagnetic systems. The electromagnetic field is an energy field, which can provide energy to electrically driven apparatus. A radiating electromagnetic wave contains energy, whether there is a receiver present or not, the energy of an electromagnetic wave is continuously consumed. By making use of a non-radiative magnetic field (near field) with a specific resonance frequency, when a resonator, such as an inductor/capacitor (*LC*) oscillating circuit with the same resonance frequency is present, then the electromagnetic resonance will generate energy in the oscillating circuit. As the energy gathered increases, the voltage across the inductor coil will also increase. As a result, two systems with the same inherent resonant frequency will generate strong magnetic resonance together with a strong magnetic field intensity. This received energy can then be used by a load after being appropriately converted by follow-up circuits [35].

MRC-WPT relies on a pair of resonant circuits with the same resonant frequency, one acting as a transmitter and the other as a receiver. The circuits contain coils which are placed so as to be strongly coupled via non-radiative magnetic resonance induction, enabling longer distance power transmission than inductive coupling [36]. Resonating circuits can be constructed from inductors and capacitors in two topology types, series and parallel. Considering the need for a resonator in both the transmitter (primary circuit) and receiver (secondary circuit), there are four possible topologies of circuit for an MRC-WPT system (as shown in Figure 1).

The electrical circuit used for the model consists of two separate coils of self-inductance L_1 and L_2 coupled by a mutual inductance M that describes the inductive coupling, accounting for coil properties and the distance between the coils. R_1 and R_2 are the equivalent resistances modelling the losses in the primary and secondary coils, respectively. C_1 and C_2 represent capacitors used in tandem with the inductors to create resonance. U_s represents the Alternating Current (A.C.) power supply Voltage.

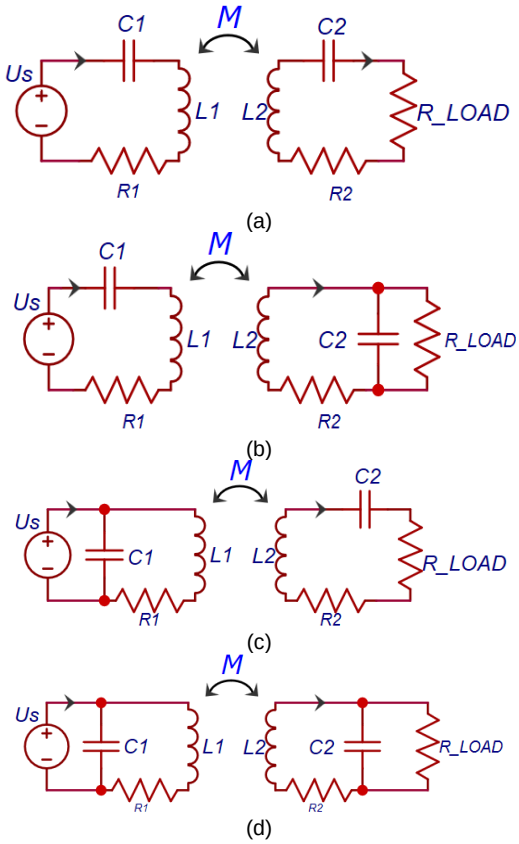

FIGURE 1 (a) Series-Series (SS) circuit (b) Series-Parallel (SP) circuit (c) Parallel-Series (PS) circuit (d) Parallel-Parallel (PP) circuit.

Each of these four topologies has advantages/disadvantages for use in the realization of a WPT system. In terms of topology selection, theoretical analysis and experimental verifications are needed to determine the most suitable choice for a WPT system. In this section, each type of primary and secondary circuit will be analysed in terms of resonant frequency and power transfer efficiency. The topologies are referred to by their parallel (P) or series (S) nature on the primary and secondary sides as and SS, SP, PP and PS.

2.1 | Series primary circuits

Topologies with a series primary circuit are first considered, i.e. SS and SP in Fig. 1(a) and 1(b) respectively.

1) Theoretical analysis

For the SS topology the equivalent impedance of the secondary circuit and the resonant frequency (ω_s), can be expressed as (1).

$$Z_{e1} = \frac{(\omega_s M)^2}{R_2 + R_L}, \quad \omega_s{}^2 = \frac{1}{L_2 C_{s2}} \tag{1}$$

If the secondary circuit is of parallel configuration, the equivalent impedance of the secondary circuit and the resonant frequency (ω_p), can be expressed as (2):

$$Z_{e2} = \frac{(\omega_p M)^2}{R_2 + \frac{L_2}{C_{p2} R_L}}, \quad \omega_p{}^2 = \frac{1}{L_2 C_{p2}} - \frac{1}{C_{p2}{}^2 R_L{}^2} \tag{2}$$

The power transfer performance depends on the equivalent impedance of the secondary circuit to that of the primary circuit at the resonant frequency [37-38]. When the equivalent impedance of the secondary circuit is larger than that of the primary circuit, the power transfer efficiency is higher. Hypothetically, the resonant frequencies are the same in both series and parallel secondary circuit configurations. In this case, the capacitance in the series secondary circuit must be different from that in parallel secondary circuit to resonate at the same frequency. Clearly, by comparing equations (1) and (2), when the load impedance R_L satisfies the condition $R_L > (L_2/C_{p2})^{0.5}$, then a parallel secondary circuit configuration should be chosen, otherwise, the series configuration is more efficient.

2.2 | Parallel Primary Circuits

Topologies with a parallel primary circuit are now considered i.e. PP and PS in Fig. 1(c) and 1(d) respectively.

In the case of the PP circuit topology, if the resistance of the inductors can be considered negligible the circuit structure can be simplified, then the equivalent input impedance can be expressed as (3).

$$Z_{in} = \frac{(1-\omega^2 L_1 C_1)[R_L(1-\omega^2 L_2 C_2) + j\omega L_2] - \omega^2 M C_1 \left(\omega^2 M C_2 R_L - j\omega M\right)}{\left(j\omega L_1\right)[R_L(1-\omega^2 L_2 C_2) + j\omega L_2] + \left(j\omega M\right)\left(\omega^2 M C_2 R_L - j\omega M\right)} \tag{3}$$

The precondition of the resonance phenomenon is that the imaginary part of the circuit input impedance goes to zero. If $L=L_1=L_2$, $C=C_1=C_2$, then the imaginary part of Z_{in} can be expressed as (4):

$$\mathrm{Im}(Z_{in}) = \frac{\omega L\left[1-\omega^2(L^2-M^2)C/L\right]\left[(1-\omega^2 LC)^2 R_L{}^2 - \omega^4 M^2 C^2 R_L{}^2 + \omega^2 L^2 - \omega^2 M^2\right]}{\left[\omega^2 L^2 - \omega^2 M^2\right]^2 + R_L{}^2\left[\omega L(1-\omega^2 LC) + \omega^3 M^2 C\right]^2} \tag{4}$$

The resonant frequency can be obtained by setting the imaginary part expressed in (3) to zero. This gives rise to:

$$f = \frac{1}{2\pi}\sqrt{\frac{L}{(L^2-M^2)C}} = \frac{1}{2\pi}\sqrt{\frac{1}{(1-k^2)LC}} \tag{5}$$

where k is the coefficient of mutual inductance. Equation (5) shows that the resonant frequency is related to k. Furthermore, the parallel topology looks like an open circuit at resonance, which results in a low current supply and hence will lead to low load power.

2.3 | Frequency splitting

Although the MRC-WPT method offers higher power transfer efficiencies than inductive coupling over a larger range [39], the phenomenon of frequency splitting can lead to reduced performance. The SS topology, as shown in Fig. 1(a), will be discussed as an example of how and when frequency splitting can occur.

I_1 and I_2 represent the currents in the primary and secondary coils respectively. U_s represents the power supply. If

$$X_1 = \omega L_1 - \frac{1}{\omega C_1} \tag{6}$$

and

$$X_2 = \omega L_2 - \frac{1}{\omega C_2} \tag{7}$$

then I_1 and I_2 can be expressed as:

$$I_1 = \frac{U_s(R_L + R_2 + jX_2)}{(R_1 + jX_1)(R_L + R_2 + jX_2) + \omega^2 M^2} \tag{8}$$

$$I_2 = \frac{j\omega M U_s}{(R_1 + jX_1)(R_L + R_2 + jX_2) + \omega^2 M^2} \tag{9}$$

The equivalent input impedance can then be expressed as:

$$\begin{aligned} Z_{in} &= R_1 + jX_1 + \frac{\omega^2 M^2}{R_L + R_2 + jX_2} \\ &= R_1 + j(\omega L_1 - \frac{1}{\omega C_1}) + \frac{\omega^2 M^2}{R_L + R_2 + j(\omega L_2 - \frac{1}{\omega C_2})} \end{aligned} \tag{10}$$

The phenomenon of resonance occurs, when the imaginary part of Z_{in} equals 0. Substituting for $L=L_1=L_2$, $C=C_1=C_2$, $\mathrm{Im}(Z_{in})$ can be expressed as:

$$\mathrm{Im}(Z_{in}) = \frac{(\omega L - \frac{1}{\omega C})\left[\left(R_L + R_2\right)^2 + (\omega L - \frac{1}{\omega C})^2 - (\omega M)^2\right]}{\left(R_L + R_2\right)^2 + (\omega L - \frac{1}{\omega C})^2} \tag{11}$$

The numerator of $\mathrm{Im}(Z_{in})$ can be separated into two factors making it easy to obtain one root for ω_0 of $(LC)^{-0.5}$ from the first factor. Equation (11) always has at least this one root, however other roots can also exist in the second factor which can be abbreviated as a two-variable linear equation:

$$y(\omega^2) = (L^2 - M^2)(\omega^2)^2 + \left[(R_2 + R_L)^2 - \frac{2L}{C}\right]\omega^2 + \frac{1}{C^2} \tag{12}$$

The angular frequency ω must be bigger than 0, which only happens when the conditions in (13) and (14) are met simultaneously.

$$\left(R_2 + R_L\right)^2 - \frac{2L}{C} \le 0 \tag{13}$$

$$\Delta = \left[\left(R_2 + R_L\right)^2 - \frac{2L}{C}\right]^2 - \frac{4(L^2 - M^2)}{C^2} \ge 0 \tag{14}$$

Now the resonance frequencies can be expressed as

$$f_{1,2}^{'} = \frac{1}{2\pi}\sqrt{\frac{-\left[\left(R_2 + R_L\right)^2 - \frac{2L}{C}\right] \pm \sqrt{\Delta}}{2(L^2 - M^2)}} \tag{15}$$

For the SS circuit, when the load resistance is large enough, there is only one resonant frequency, which can be directly calculated from the inductance and capacitance as in (1). In this case, however, the power transfer efficiency is low. When the

load resistance is small enough to meet the condition of equation (13), multiple resonant frequencies will appear and the value of those resonant frequencies is related to the mutual inductance. Several conditions can be summarized as shown in TABLE I. From equation (14), when the mutual inductance is large, the value of Δ is greater than 0, making it easy to get multiple resonant frequencies. However, the power transfer efficiency and load power cannot reach their maximum potential at all of these resonant frequencies.

TABLE I CALCULATED RESONANCE FREQUENCIES WITH DIFFERENT CONDITIONS IN AN SS CIRCUIT

Conditions		Resonance Frequencies
$(R_2+R_L)^2-\frac{2L}{C}\geq 0$		$f_1=\frac{1}{2\pi\sqrt{LC}}$
$(R_2+R_L)^2-\frac{2L}{C}<0$	$\Delta<0$	$f_1=\frac{1}{2\pi\sqrt{LC}}$
	$\Delta=0$	$f_1=\frac{1}{2\pi\sqrt{LC}}$ $f_2=\frac{1}{2\pi}\sqrt{\frac{-\left[(R_2+R_L)^2-\frac{2L}{C}\right]}{2(L^2-M^2)}}$
	$\Delta>0$	$f_1=\frac{1}{2\pi\sqrt{LC}}$ $f_{2,3}=\frac{1}{2\pi}\sqrt{\frac{-\left[(R_2+R_L)^2-\frac{2L}{C}\right]\pm\sqrt{\left[(R_2+R_L)^2-\frac{2L}{C}\right]^2-\frac{4(L^2-M^2)}{C^2}}}{2(L^2-M^2)}}$

TABLE II QUALITATIVE COMPARISONS OF THE FOUR TOPOLOGIES.

Topologies	Features
SS	1.Equal to short circuit at resonance frequency 2.Suitable for load impedance less than $(L_2/C_2)^{0.5}$ 3. Large current in the circuits 4. The phenomenon of frequency splitting
SP	1.Equal to open circuit at resonance frequency 2.Suitable for load impedance larger than $(L_2/C_2)^{0.5}$ 3. Large voltage in the secondary circuit 4.The compensated capacitance is related to load
PS	1.Equal to open circuit at resonance frequency 2.Suitable for load impedance less than $(L_2/C_2)^{0.5}$ Tiny current in the circuits 2.Tiny load power 3.The resonance frequency is affected by mutual inductance
PP	1.Equal to open circuit at resonance frequency 2.Suitable for load impedance larger than $(L_2/C_2)^{0.5}$ 3.Tiny current in the circuits 4.Tiny load power 5.The resonance frequency is affected by mutual inductance 6.The compensated capacitance is related to load and mutual inductance

Although the SS circuit is suitable for small loads, frequency splitting makes the topology difficult in application. Only when all parameters satisfy the condition Δ<0, do both the power transfer efficiency and the load power reach their maximums. Comparisons of the four topologies are provided in TABLE II.

3 | EXPERIMENTAL SETUP

According to the theoretical analysis, solutions for designing an optimal WPT system are shown in Figure 2 for an application with a fixed load. Firstly, the load impedance needs to be defined for different applications. Secondly, the inductances and capacitances need to be determined based on the fixed load and finally the topology of secondary circuit for WPT needs to be considered. To compare the difference between the two topologies of primary circuit, experimental results need to be obtained. Finally, a WPT design is proposed with optimised parameters to gain both high load power and power transfer efficiency and avoid the phenomenon of frequency splitting.

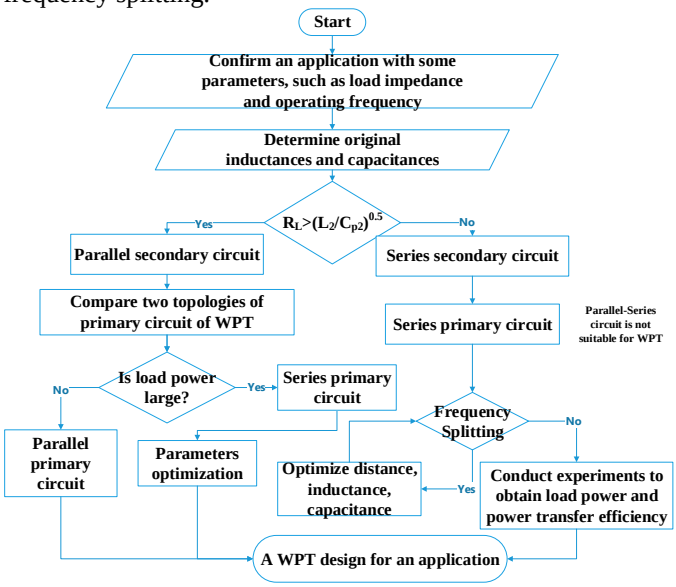

FIGURE 2 A flow chart to design a WPT system.

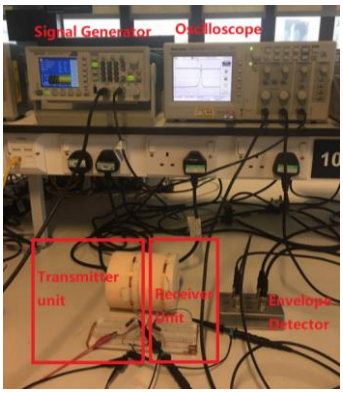

FIGURE 3 Experimental setup of WPT circuit.

To conduct experimental verification, two coils were manufactured to form inductors each with 10 turns and a radius of 5 cm. The inductance of the coils was measured to be 25.2 uH using a multi-frequency LCR meter. The resistance of the coils was measured to be 0.73 Ω. The distance between the

two coils was fixed at 5 cm. The capacitances of the capacitors were calculated using the equations in [35] for WPT operation at 6.78 MHz, which is in an unlicensed band. The experimental setup is shown in Figure 3.

Currents and voltages were measured at various points around the circuits and at the load using a multi-meter and an oscilloscope to allow load power and input power to be calculated. The power transfer efficiency can be calculated by (16).

$$\eta=\frac{\mathbf{P}_{load}}{\mathbf{P}_{in}}\times 100\%=\frac{I_{out}^{2}R_{load}}{\dot{U}_{s}\dot{I}_{s}}\times 100\% \qquad (16)$$

4 | EXPERIMENTAL VERIFICATION

4.1 | Effected by fixed load

The SS and SP circuits for WPT were constructed as shown in Fig. 1(a) and 1(b). To investigate the influence of load impedance, the load was varied as: 100 Ω, 500 Ω, 1.6 kΩ, 5 kΩ and 10 kΩ, which represent the fixed load impedances of some sensors and electrical devices [40-41].

From Figure 4, it is seen that the experimental results show good agreement with the theoretical results for both the SS and SP topologies. When the load impedance is smaller than 1.6 kΩ, the power transfer efficiency at 6.78 MHz in the SS topology is higher than that of the SP topology. However, when the load impedance is larger than 1.6 kΩ, the power transfer efficiency in the SP topology is higher than that in the SS topology. What's more, the power transfer efficiency reaches over 80% for small load impedances in the SS topology, whereas similar efficiencies are seen for large load impedances in the SP topology.

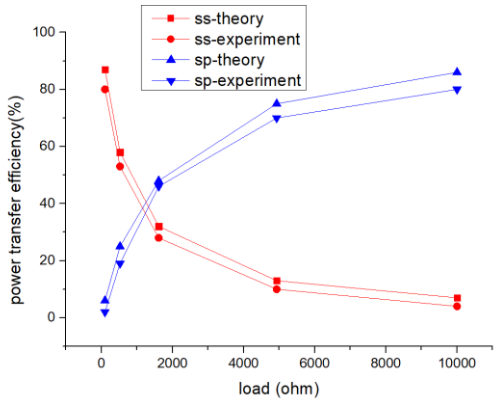

FIGURE 4 Theoretical and experimental power transfer efficiency in SS and SP topologies for varying loads

Therefore, a series secondary circuit is suitable for a system delivering power to a small load, whereas a parallel secondary circuit is suitable for a system delivering power to a large load in order to enhance power transfer efficiency.

4.2 | Load power comparisons

Using the experimental system as defined in Section 3, with the distance set at 5 cm the mutual inductance of the coils was measured to be k=2.115 uH. The theoretical resonant frequency of this WPT circuit shifts from 6.78 MHz to 6.83 MHz. The load impedance is 5 kΩ.

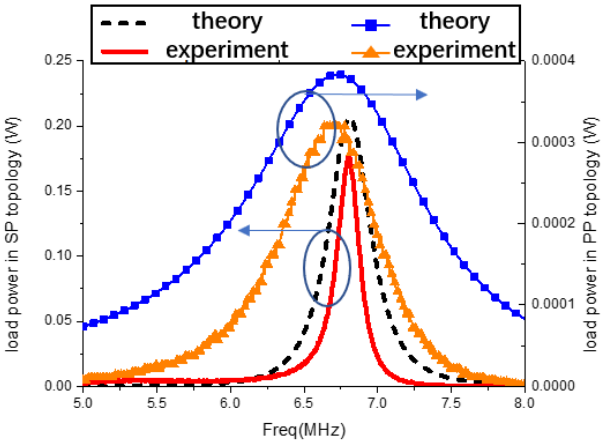

FIGURE 5 Comparison of load power against frequency from theoretical and experimental results for (a) PP topology and (b) SP topology

Figure 5(a) shows that the power delivered to the load is only 0.33 uW at the resonant frequency in the PP topology whereas the load power can reach 0.17 W at the resonant frequency in SP topology as shown in Figure 5(b).

The parallel primary circuit provides high power transfer efficiency over a large distance, however the load power obtained is tiny, compared with that obtained from the series primary circuit. Independent of the primary circuit type, a series secondary circuit is suitable for small loads and a parallel secondary circuit is suitable for large loads. The theoretical analysis here is similar to that shown in section IV.A. The PS topology can obtain high power transfer efficiency over a large distance only for a small load, but the load power is on the order of micro Watts. Therefore, it is more appropriate to use a series topology for the primary circuit of the WPT system to maximize load power and high power transfer efficiency.

The series primary circuit has been shown to transfer larger power, however, it is necessary to avoid the associated phenomenon of, frequency splitting. This can result in high power transfer efficiency but not maximized load power. In the following section, circuit theory and experiments are used to explain and demonstrate the frequency splitting phenomenon.

4.3 | Optimization

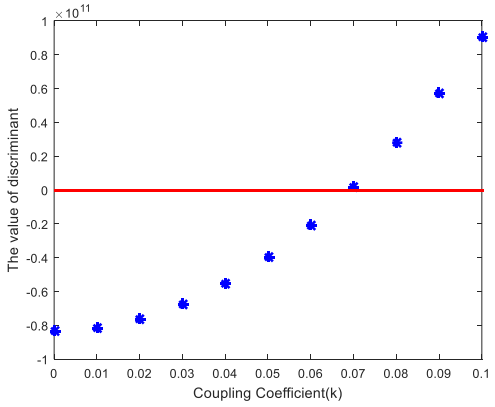

FIGURE 6 The value of Δ with the varying coefficient

When the load impedance is 100 Ω, equation (14) is satisfied, and the value of Δ varies with the coupling coefficient as shown in Figure 6. The coefficient of mutual inductance is 0.084 when the distance between the two coils is 5 cm. In this case, the value of Δ is greater than 0, which means there are three resonant frequencies.

Trends of load power and power transfer efficiency against frequency are shown in Figure 7. The load power reaches two peaks at two of the resonant frequencies, however the power transfer efficiency is not maximum in either case. Conversely, the power transfer efficiency reaches a peak where the load power drops into the valley point between the peaks.

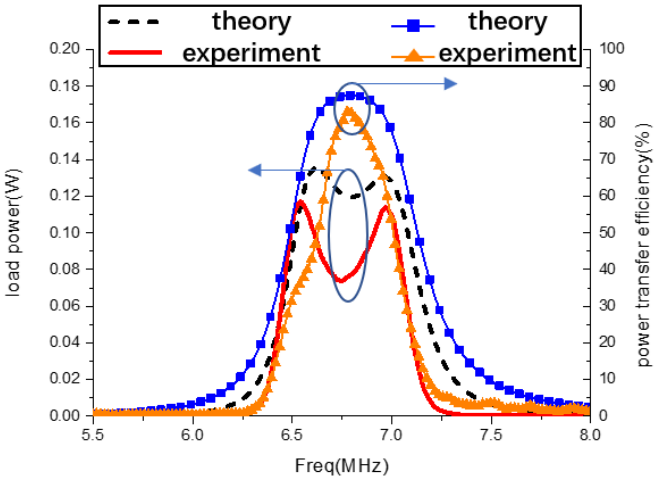

FIGURE 7 Trends of the load power and the power transfer efficiency against frequency showing the phenomenon of frequency splitting.

When the distance between the two coils reaches 8 cm, the coupling coefficient is 0.05, in this case, the value of Δ is less than 0 and there is only one resonant frequency. Trends of load power and power transfer efficiency against frequency are shown in Figure 8. Both the load power and power transfer efficiency reach their peak at this one resonant frequency.

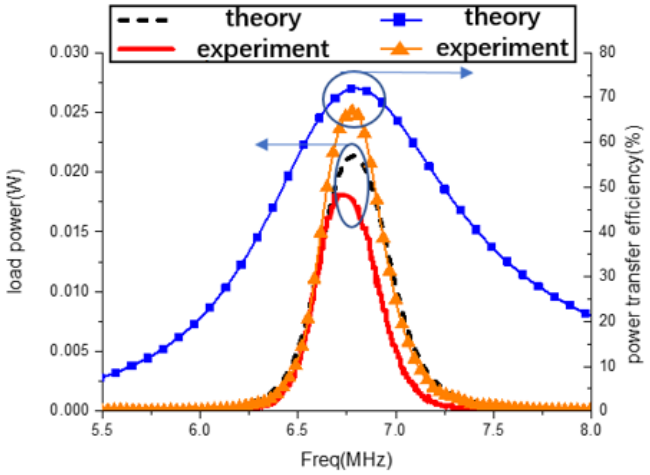

FIGURE 8 Trends of load power and power transfer efficiency against frequency without the phenomenon of frequency splitting by increasing transfer distance

When the load impedance is 5 kΩ, equation (14) is not satisfied, and hence there is only one resonant frequency as well. The trends of load power and power transfer efficiency with varying frequency are shown in Figure 9. Both the load power and power transfer efficiency reach their peak at the one resonant frequency.

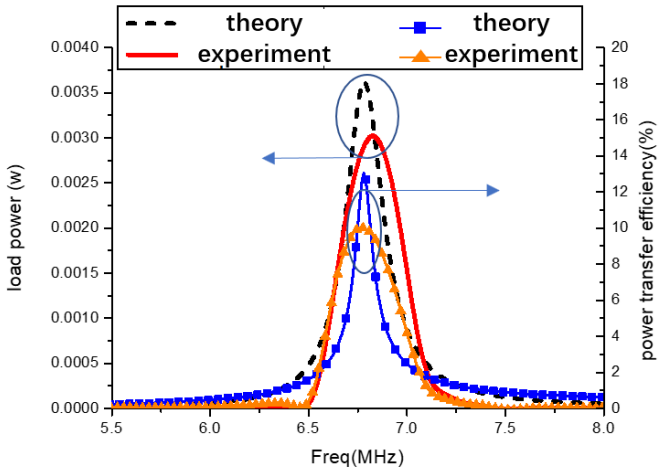

FIGURE 9 Trends of load power and power transfer efficiency with varying of frequency without the phenomenon of frequency splitting by changing load impedance

Although SS topologies are suitable for small loads, they often lead to the phenomenon of frequency splitting, especially, when the distance between coils is short. To avoid this phenomenon, the distance could be made larger, however, the load power and the power transfer efficiency will decrease. Consequently, there is a trade-off between load power, load and distance.

5 | CONCLUSION

An investigation of the four possible system topologies for magnetic resonance coupling for wireless power transfer has been presented in terms of both theoretical analysis and experimental verification. Application of a series secondary circuit was shown to be suitable for power transfer to small loads, however, if the load impedance is large then the parallel secondary circuit is more appropriate. For the primary circuit the parallel topology looks like an open circuit at resonance, which means a low current will be supplied to the inductor. Consequently, the power transferred to the secondary circuit will be low making it inappropriate for use in WPT applications.

The resonance frequency is affected by mutual inductance which is itself affected as the distance and/or environment between the coils changes. As the distance or environment changes the resonance frequency will be shifted, resulting in the load power and power transfer efficiency being reduced.

For the SS topology, the phenomenon of frequency splitting should be avoided to maintain maximum load power and power transfer efficiency at resonance. Only when the load impedance and transfer distance are carefully chosen, can the load power and power transfer efficiency maintain their maximums at resonance, but in this case, the power transfer is not very high.

Finally, the SP topology is shown to be the most suitable candidate for use in wireless power transfer. Inductances, capacitances and the load impedances need to be optimized in order to gain maximum load power and transfer efficiency for the maximum transfer distance.

REFERENCES

[1] T. Campi, S. Cruciani, F. Palandrani, V. De Santis, A. Hirata, and M. Feliziani, "Wireless power transfer charging system for AIMDs and pacemakers," *IEEE Transactions on Microwave Theory and Techniques*, vol. 64, no. 2, pp. 633-642. Feb. 2016

[2] Kyungmin Na, Heedon Jang, Hyunggun Ma, and Franklin Bien, "Tracking Optimal Efficiency of Magnetic Resonance Wireless Power Transfer System for Biomedical Capsule Endoscopy", *IEEE Transactions on Microwave Theory and Techniques*, vol. 63, no. 1, pp. 295-303, Jan. 2015

[3] Guizhi Xu, Xinsheng Yang, Qingxin Yang, Jun Zhao, and Yang Li, "Design on Magnetic Coupling Resonance Wireless Energy Transmission and Monitoring System for Implanted Devices", *IEEE Trans. Applied Superconductivity*, vol. 26. no.4, pp. 4400804, June.2016.

[4] R. Wu, W. Li, H. Luo; J. K. Sin and C. P. Yue, "Design and characterization of wireless power links for brain-machine interface applications", *IEEE Transaction on Power Electronics*. vol.29, pp. 5462-5471, 2014

[5] C. Liu, K. T. Zhang, Z. Zhang, C. Qiu, W. Li, and T. Ching, "Wireless power transfer and fault diagnosis of high-voltage power line via robotic bird", *Journal of Applied Physics*, vol.117, no.17, pp. 1-4, 2015

[6] Duc. Hung. Tran, Van. Binh. Vu and Woojin. Choi, "Design of a high-efficiency wireless power transfer system with intermediate coils for the on-board chargers of electric vehicles," *IEEE Transactions on power electronics*. vol. 33, no. 1, pp. 175-187, Jan. 2018

[7] Mariusz. Bojarski, Erdem. Asa, Kerim. Colak and Dariusz. Czarkowski, "Analysis and control of multiphase inductively coupled resonant converter for wireless electric vehicle charger application," *IEEE Transactions on transportation electrification*, vol. 3, no.2, pp. 312-320, June, 2017.

[8] K. Hwang, J. Cho, D. Kim, J. Park; J. K. Kwon, S. I. Kwak, H. H. Park and S. Ahn, "An autonomous coil alignment system for the dynamic wireless charging of electric vehicles to minimize lateral misalignment", Energies, vol. 10. no.3, pp.315, 2017

[9] Jiejian Dai, Daniel C. Ludois. A survey of Wireless Power Transfer and a Critical Comparison of Inductive and Capacitive Coupling for Small Gap Application., *IEEE Transaction on Power Electronics*, vol.30, no.11, pp.6017-6029. 2015.

[10] A. M. Jawad, R. Nordin, S. K. Gharghan, H. M. Jawad and M. Ismail, "Opportunities and challenges for near-field wireless power transfer: a review", *Energies*, vol.10, no.7, pp.1-28, July 2017

[11] H. Dinis, I. Colmiais and P. M. Mendes, "Extending the limits of wireless power transfer to miniaturized implanted electronic devices", *Micromachines*, vol. 8, no.12, pp.1-15, Dec 2017

[12] Andre. Kurs, Aristeidis. Karalis, Robert. Moffatt, J. D. Joannopoulos, Peter. Fisher, and Marin. Soljacic, Wireless Power Transfer via Strongly Coupled Magnetic Resonance. *Science*, vol. 317, no. 6, pp. 83-86. 2007.

[13] Mingzhao. Song, Pavel Belov and Polina Kapitanova. "Wireless power transfer inspired by the modern trends in electromagnetics", *Applied Physics Review*, vol. 4. no.2 pp.1-18, 2017

[14] Dowon Kim, Ahmed Abu-Siada and Adrian Sutinjo, "State-of-the-art literature review of WPT: Current limitations and solutions on IPT", *Electric Power Systems Research*, vol. 154, pp.493-502, 2018

[15] Wencheng. Lu, Xiaohui. Qiu, Xingkui. Mao and Wei. Chen, "Comparison of series series model and series parallel model of wireless power transmission via magnetic resonance," *Power electronics*, vol. 49, no. 10, pp.73-76, Oct. 2015.

[16] R. Jegadeesan and Y. X. Guo, "Topology Selection and Efficiency Improvement of Inductive Power Links", *IEEE Transactions on Antenna and Propagation*, vol. 60, no. 10, pp.4846-4854, Oct. 2012.

[17] W. Zhang, S. C. Wong, K. T. Chi and Q. Chen, "Analysis and comparison of secondary series-and parallel-compensated inductive power transfer systems operating for optimal efficiency and load-independent voltage-transfer ratio", *IEEE Transactions on Power Electronics*, vol.29, no.6, pp.2979-2990, Jun 2014.

[18] Hongwei. Zhou, Liping. Sun, Shuai. Wang, Tianshi. Liu and Penghao. Xie, "Resonant model analysis of wireless power transfer via magnetic resonant coupling", *Electric machines and control*. Vol. 20, no. 7, pp. 65-73. July, 2016

[19] C. Xiao, K. Wei, F. Liu and Y. Ma, "Matching capacitance and transfer efficiency of four wireless power transfer systems via magnetic coupling resonance", *International Journal of Circuit Theory and Applications*, vol.45, no.6, pp. 811-831, Jun 2017

[20] C. Jiang, K. T. Chau, C. Liu and C. H. T. Lee, "An overview of resonant circuits for wireless power transfer", *Energies*, vol.10, no.7, pp.1-20, Jul 2017.

[21] Y. Yi, U. Butter, Y. Fan and I. G. Foulds, "Design and optimization of a 3-coil resonance-based wireless power transfer system for biomedical implants", *International Journal of Circuit Theory and Applications*, vol. 43, no.10, pp.1379-1390, Oct 2015.

[22] U. Jow, M. Ghovanloo, "Design and optimization of printed spiral coils for efficient transcutaneous inductive power transmission", *IEEE Transactions on Biomedical Circuits and System*, vol.1. no.3, pp.193-202, Sep 2007.

[23] H. Qiang, X. Huang, L. Tan, Q. Ji and J. Zhao, "Achieving maximum power transfer of inductively coupled wireless power transfer system based on dynamic tuning control", *Science China-Technological Sciences*, vol.55, no.7, pp.1886-1893, Jul 2012

[24] W. Lu, M. Zhao, L. Zhou, H. H. C. Iu and J. Zhao, "Modeling and analysis of magnetically coupled resonance wireless power transfer system with rectifier bridge LED load", *International Journal of Circuit Theory and Applications*, vol.43, no.12, pp.1914-1924, Dec 2015

[25] J. Kim and J. Jeon, "Range-adaptive wireless power transfer using multiloop and tunable matching techniques", *IEEE Transactions on Industrial Electronics*, vol.62, no.10, pp.6233-6241, 2015.

[26] H. Feng, T. Cai, S. Duan and X. Zhang, H. Hu and J. Niu, "A dual-side-detuned series-series compensated resonant converter for wide charging region in a wireless power transfer system", *IEEE Transactions on Industrial Electronics*, vol.65, no.3, pp. 2177-2188, March 2018.

[27] Y. Lyu, F. Meng, G. Yang, B. Che, Q. Wu, L. Sun, D. Emi and J. L. Li, "A method of using nonidentical resonant coils for frequency splitting elimination in wireless power transfer", *IEEE Transactions on Power Electronics*, vol.30, no.11, pp.6097-6107, Nov. 2015.

[28] R. Huang, B. Zhang, D. Qiu and Y. Zhang, "Frequency splitting phenomena of magnetic resonant coupling wireless power transfer", *IEEE Transactions on Magnetics*, vol.50, no.11, pp.1-4, Dec 2014

[29] N.C. Kuo, B. Zhao and A.M. Niknejad, "Bifurcation analysis in weakly-coupled inductive power transfer systems", *IEEE Transactions on Circuits and Systems I-Regular Papers*, vol.63, no.5, pp.727-738, May 2016

[30] N. Inagaki, "Theory of image impedance matching for inductively coupled power transfer systems", *IEEE transactions on Microwave Theory and Techniques*, vol.62. no.4, pp.901-908, 2014

[31] Y. Lim, H. Tang, S. Lim and S. Park, "An adaptive impedance matching network based on a novel capacitor-matrix for wireless power tranfer", *IEEE Transactions on Power Electronics*, vol.29, no.8, pp.4403-4413, 2014

[32] M. Catrysse, B. Hermans, R. Puers, "An inductive power system with integrated bidirectional data-transmission", *Sensors and Actuators A-Physical*, vol.115, no.2-3, pp. 221-229, Sep 2014

[33] F. Jolani, Y. Yu and Z. Chen, "A planar magnetically coupled resonant wireless power transfer using printed spiral coils", *IEEE Antenna Wireless Propagation Letter*, vol.13, pp. 1648-1651, Aug 2014

[34] Yingman. Chen, Dazhong. Wu and Hongyu. Wang, "Experimental study of parameter optimization in wireless power transmission system based on magnetic resonant coupling," *Experimental technology and management*, vol. 33, no. 8, pp. 32-36, Aug. 2016.

[35] Chunbo Zhu, Kai Liu, Chunlai Yu, Rui Ma, Hexiao Cheng. "Simulation and experimental analysis on wireless energy transfer based on magnetic resonances". *IEEE Vehicle Power and Propulsion Conference (VPPC)*, Harbin, China, pp. 1-4, 2008.

[36] Liang Xie, Yi Shi, Y. Thomas Hou and Wenjing Lou. Wireless Power Transfer and Application to Sensor Networks. *IEEE Wireless Communications*, 2013. vol. 20, no. 4, pp. 140-145.

[37] M. Kiani, M. Ghovanloo, "The circuit theory behind coupled-mode magnetic resonance-based wireless power transmission", *IEEE Transactions on Circuits and System I-Regular Papers*, vol. 59, no.9, pp.2065-2074, Sep 2012

[38] A. A. Eteng, S. K. A. Rahim, C. Y. Leow, S. Jayaprakasam, "Low-power near-field magnetic wireless energy transfer links: a review of

architectures and design approaches", *Renewable and Sustainable Energy Reviews*, vol.77, pp.486-505, Sep 2017.

[39] Kush Agarwal, Rangarajan Jegadeesan, Yongxin. Guo, Nitish V. Thakor, "Wireless power transfer strategies for implantable bioelectronics: Methodological Review", *IEEE Reviews in Biomedical Engineering*, vol. 10, pp.1-28, 2017.

[40] D. A. Borton, M. Yin, J. Aceros and A. Nurmikko, "An implantable wireless neural interface for recording cortical circuit dynamics in moving primates", *Journal of Neural Engineering*, vol. 10. No.2, pp. 026010, Feb 2013

[41] E. F. Kilinc, C. Dehollain and F. Maloberti, "Remote powering and data communication for implanted biomedical systems", *Analog Circuits and Signal Processing*; Switzerland: Springer, 2016